others. The total cross section for production of observable strange particles by protons increases more rapidly with A, from C to Pb, than in the case of production by pions. The lower cross section and more rapid variation with A indicate that indirect production of strange particles by intermediate pions accounts for a significant fraction of all strange particles produced by protons, even in carbon. An estimate of the total proton-nucleon direct production of observable strange particles ($\Lambda^0, \theta_1^0, \Sigma_\pi^\pm \rightarrow \pi^\pm + n$) giving a reasonable fit to the observed cross sections is 0.09 ± 0.06 mb.

A comparison of the cloud chamber results with the γ-ray yields observed at 90° from points downstream from Cosmotron targets indicates satisfactory agreement between the results of the two entirely different techniques of observing strange particle production. This strengthens the evidence that the γ rays are indeed the result of strange particle decays. The observed A dependence is in good agreement, giving greater weight to the cloud-chamber evidence that strange-particle production increases more rapidly with A than the total inelastic cross section from C to Pb.

It is hoped that the angular and momentum distributions will serve as a guide to those who contemplate experiments making use of strange particles produced by ≈3-Bev protons. Preliminary results from a Monte Carlo calculation carried out on the Los Alamos Maniac II[26] indicate that the present results on complex nuclei can be understood in terms of a cascade of individual particle-nucleon collisions with nucleons within the nucleus. The reliability of such a calculation to predict strange particle production from a proton-nucleus collision should improve as more observations are made of p-p and p-d collisions, and as more is known about strange-particle nucleon interactions. Proton-nucleus collisions at ≈3 Bev are not as suitable as pion-nucleus collisions for gaining information about strange-particle nucleon interactions, since the production cross sections are smaller, and the cascade of nuclear collisions involved is more complicated.

ACKNOWLEDGMENTS

In addition to the many persons to whom we are greatly indebted who are mentioned in I, we would also like to acknowledge the help of Dr. C. R. Sun. Dr. E. Boldt kindly supplied us with information about the MIT proton-produced events, and we benefited from discussions with Dr. G. B. Collins and Dr. D. Berley concerning the details of their γ-ray counting experiment.

[26] L. Sartori, A. E. Werbrouck, J. K. Wooten, and R. L. Bivins, Bull. Am. Phys. Soc. 4, 289 (1959).

PHYSICAL REVIEW VOLUME 119, NUMBER 6 SEPTEMBER 15, 1960

Branching Ratio of the Electronic Mode of Positive Pion Decay*

H. L. ANDERSON, T. FUJII, R. H. MILLER,† AND L. TAU‡
The Enrico Fermi Institute for Nuclear Studies, The University of Chicago, Chicago, Illinois

(Received May 13, 1960)

A new measurement of the branching ratio $(\pi^+ \rightarrow e^+ + \nu)/(\pi^+ \rightarrow \mu^+ + \nu)$ has been completed. A double-focussing magnetic spectrometer was used to observe the spectra of electrons emitted in π decay and in μ decay. The scintillation pulses from the pion and its decay electron were recorded on a travelling-wave oscilloscope. Timing and pulse-height measurements were used to distinguish good events from accidentals. The total number of π-e events recorded in this experiment was 1346, of which 6% were accidentals and 5% were π-μ-e contamination. The branching ratio obtained from an analysis of the data over the π-e and μ-e distributions and corrected to include all decay electrons was $(1.21 \pm 0.07) \times 10^{-4}$. This is close to the result expected for a universal V-A interaction. Kinoshita's calculation, taking into account radiative effects, gave 1.23×10^{-4}. Our data also gave for the mean life of π decay $\tau_\pi = (25.6 \pm 0.8) \times 10^{-9}$ second.

INTRODUCTION

THE charged pion normally decays into a muon and a light neutral particle, presumed to be a neutrino. The alternative decay mode, into an electron instead of a muon, was shown by earlier measurements to have a small branching ratio. Friedman and Rainwater[1] examining pion endings in photographic emulsion could report zero or one such decay in 1419 muonic decays. Subsequently, Lokanathan and Steinberger,[2] using a counter telescope arrangement, sensitive to the higher energy and shorter lifetime of the π decay to discriminate against the electrons from μ decay, reported a branching ratio $f = (-3 \pm 9) \times 10^{-5}$. In this laboratory, Anderson and Lattes[3] using a magnetic spectrometer to single out the electrons of π decay also failed to find the electronic mode. They reported a

* Research performed under the joint sponsorship of the Office of Naval Research and the U. S. Atomic Energy Commission.

† Now at Yerkes Observatory, the University of Chicago, Chicago, Illinois.

‡ Now at Institute of Physics, University of Rome, Rome, Italy.

[1] H. L. Friedman and J. Rainwater, Phys. Rev. 84, 684 (1949).

[2] S. Lokanathan and J. Steinberger, Suppl. Nuovo cimento 1, 151 (1955).

[3] H. L. Anderson and C. M. G. Lattes, Nuovo cimento 6, 1356 (1957).

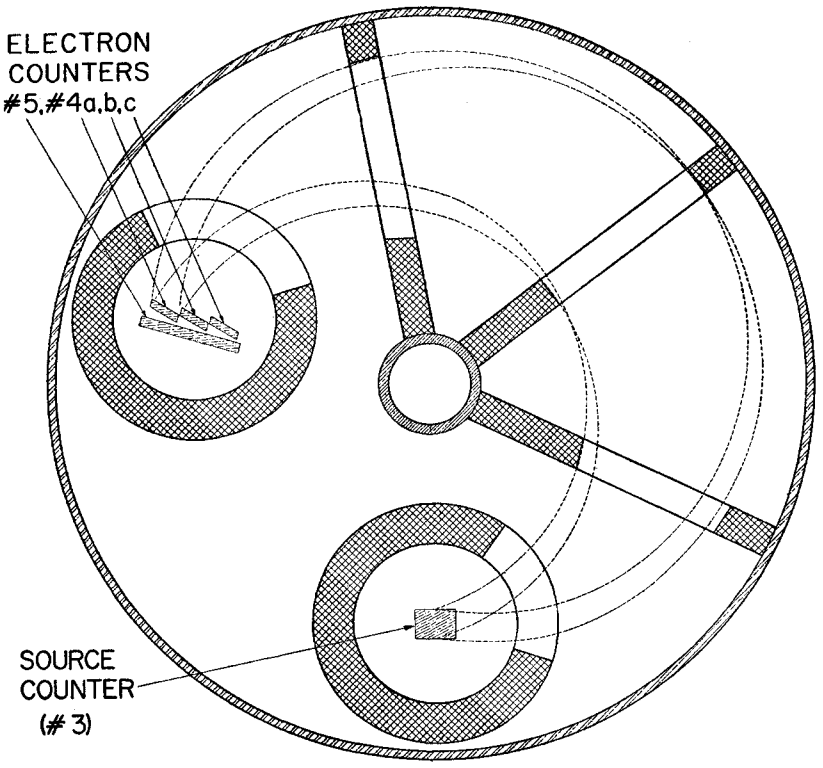

FIG. 1. Sectional view of double focussing spectrometer with three momentum channels. Extreme trajectories in one of the channels are indicated by dotted lines.

branching ratio $f=(0.4\pm9.0)\times10^{-6}$. This result was placed in doubt when Feynman and Gell-Mann[4] and Sudarshan and Marshak[5] found it to be inconsistent with an estimate of the branching ratio based on a universal A-V beta interaction, otherwise highly successful in accounting for a wide range of related phenomena. The A-V theory predicts a value close to 1.2×10^{-4} for the branching ratio, the exact value depending on the extent to which the observations include the effects of radiative processes.[6,7] New attempts to observe the electronic mode proved successful. Positive evidence for the existence of the π-e mode with the expected frequency was first announced by the CERN group[8] who used an improved counter telescope in their experiment. At the same time the Columbia group[9] was able to publish photographs of π-e events taken in their hydrogen bubble chamber, in confirmation of the CERN announcement. A preliminary measurement by the present authors,[10] using a magnetic spectrometer, gave for the branching ratio the value $f=(1.03\pm0.20)\times10^{-4}$. Comparable observations by Crowe et al.[11] and by DeStaebler, Richter, and Panofsky[12] have been reported but not yet published. The earlier report from this laboratory[3] that the branching ratio was less than 10^{-4} turned out to be incorrect. The difficulty with this experiment is discussed below.

We report here a new experiment undertaken to obtain as accurate a measure of the branching ratio as our present equipment and facilities would allow. The duty cycle of the cyclotron was increased five-fold and at the same time the intensity, focussing, and energy homogeneity of the pion beam were improved to such an extent that we were able to record 10 π-e events per hour at the optimum current setting of the spectrometer, one in every 2×10^6 of the pions reaching the target in the spectrometer. The electronic circuitry was rebuilt, using new high speed diodes and transistors. The coincidence circuits were faster than those used previously and operated more reliably. The amplitude and shape of the pulses were improved so that each event which was recorded on a travelling wave oscilloscope could be measured with higher accuracy. The total number of π-e events recorded in this experiment was 1346, ten times that obtained previously. Of these, only 6% were accidental coincidences and 5% were

[4] R. P. Feynmann and M. Gell-Mann, Phys. Rev. **109**, 193 (1958).
[5] E. C. G. Sudarshan and R. E. Marshak, Phys. Rev. **109**, 1860 (1958).
[6] S. M. Berman, Phys. Rev. Letters **1**, 468 (1958).
[7] T. Kinoshita, Phys. Rev. Letters **2**, 477 (1959).
[8] T. Fazzini, G. Fidecaro, A. W. Merrison, H. Paul, and A. V. Tollestrup, Phys. Rev. Letters **1**, 247 (1958); J. Ashkin, T. Fazzini, G. Fidecaro, A. W. Merrison, H. Paul, and A. V. Tollestrup, Nuovo cimento **8**, 1240 (1959).
[9] G. Impeduglia, R. Plano, A. Prodell, N. Samios, M. Schwartz, and J. Steinberger, Phys. Rev. Letters **1**, 249 (1958).
[10] H. L. Anderson, T. Fujii, R. H. Miller, and L. Tau, Phys. Rev. Letters **2**, 53 (1959).
[11] K. M. Crowe (private communication).
[12] H. C. DeStaebler, Jr., B. Richter, and W. K. H. Panofsky (private communication).

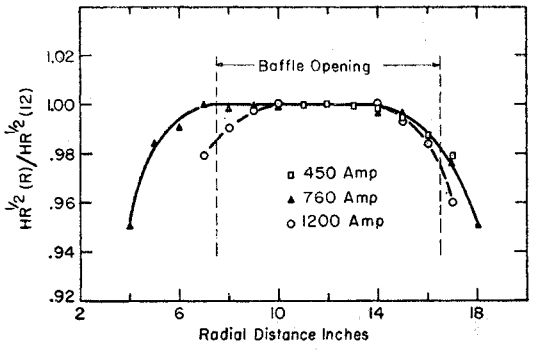

FIG. 2. Radial behavior of the magnetic field at 450, 760, and 1200 amperes. The plots give the radial variations of the quantity $IIR^{\frac{1}{2}}$. All points are shown only where differences were apparent. In the region between the extreme trajectories, indicated by the vertical dotted lines, no difference between the 450 and 760 ampere data was found. Some effect of saturation is evident at 1200 amperes.

π-μ-e contamination. There were very few ambiguous events.

SPECTROMETER

We used the same double focussing magnetic spectrometer as in the earlier work[3] to select the electrons from π decay, energy $E_\pi = 69.8$ Mev, and distinguish them from those from μ decay which have a maximum energy $E_{\mu\,\max} = 52.9$ Mev. This spectrometer has a central orbit radius of 12 inches, and is capable of focussing electrons of momentum up to 110 Mev/c. The spectrometer was modified as shown in Fig. 1. The baffling was altered to accommodate the trajectories for three detectors, covering three adjacent momentum channels. The limiting aperture was set by the central baffle which had a square opening, 9 inches in the radial direction and 9 inches in the axial direction. The scintillators 4a, b, c were made sensitive to α particles by overlaying the front surfaces of these with clear cesium iodide single crystals $\frac{1}{2}$ mm thick.

Measurements of the radial behavior of the magnetic field are given in Fig. 2, which shows a dependence quite close to $r^{-\frac{1}{2}}$, at least over the region actually used. The characteristics of a spectrometer with such a magnetic field behavior may be calculated using the formulas derived by Siegbahn and Svartholm.[13] In general, the behavior of the spectrometer was in good accord with what could be expected on the basis of these formulas.

The spectrometer was calibrated using a Pu^{239} α-particle source kindly prepared for us by Mr. Ray Brown of the Argonne National Laboratory. This source emitted α particles almost uniformly over the region in which most of the pions came to rest. This region extended $1\frac{1}{2}$ inches radially and 2 inches azimuthally in the spectrometer. Because the source was inclined at 45° to the axis of the spectrometer to permit the use of thinner pion targets, it also extended 2 inches in the axial direction. The response of the spectrometer to these α particles in the various channels is shown in Fig. 3. The source was measured and found to emit 1.02×10^6 α's per minute. From this the transmission of the spectrometer was obtained. It was close to 1.2% for channel a, 1.5% for b, and 1.6% for c. These values are somewhat less than the maximum, 2.2% accepted by the baffles because of aberrations in the focussing and the finite extensions of source and detector.[13]

The resolution width was largely limited by the radial extension of the detector. The full width at half maximum turned out to be 3.4% with the 1.5-inch wide source. This result may be obtained from Fig. 3 once the magnetic field calibration is applied to the values of magnet current given there. It is only slightly more than can be accounted for by the widths of the source and the detector alone. Measurements with a smaller source ($\frac{1}{2}$ in.$\times$1 in.) emitting 1.06×10^6 α's per minute gave higher transmissions 1.6%, 1.8%, and 1.9% for a, b, and c, respectively. There was not much reduction

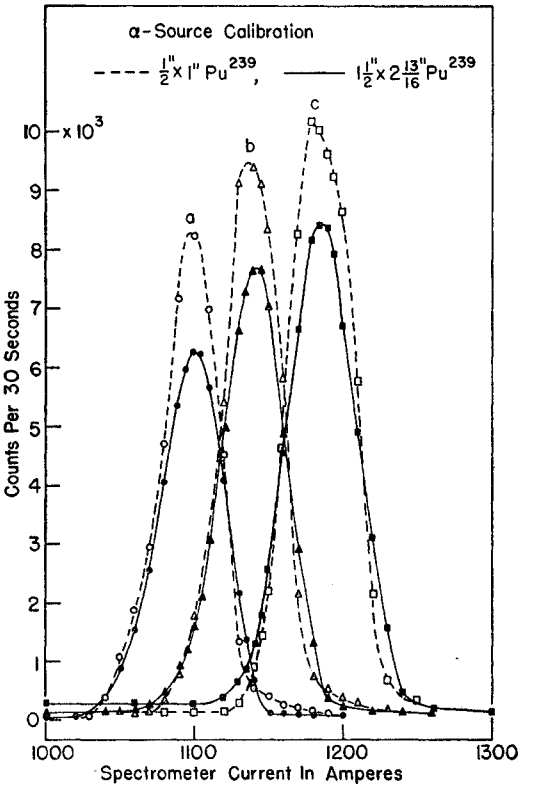

FIG. 3. Response of the spectrometer to α particles from Pu^{239} in the three channels a, b and c. Solid curves refer to a source 1.5 in.$\times$2.83 in., the same size as the target, emitting 1.02×10^6 α's per minute. The dotted curves refer to a smaller source 0.5 in.$\times$1 in. emitting 1.06×10^6 α's per minute.

[13] N. Svartholm and K. Siegbahn, Arkiv. Mat. Astron. Fysik **33A** 21 (1947); N. Svartholm, Arkiv. Mat. Astron. Fysik **33A**, 24 (1947); P. H. Stoker, O. Ping Hok, E. F. de Haan, and G. J. Sizoo, Physica **20**, 337 (1954); E. Arbman and N. Svartholm, Arkiv. Fysik **10**, 1 (1955). For a review and other references, see E. Persico and B. Geoffrion, Rev. Sci. Instr. **21**, 945 (1950).

in the resolution width, showing that the resolution function of the spectrometer will not be much affected by nonuniformities in the distribution of stopping pions in the spectrometer.

The α-particle curves were used in the interpretation of the observed response of the spectrometer to the electrons in the experiment. For this purpose the useful function $G(\xi)$ with $\xi=(p-p_0)/p_0$ was derived from the α-particle data. It was assumed to be independent of the momentum p_0 at which the spectrometer was set. There is such a function for each channel. These functions, tabulated in Table I, were based on the observations with the larger source.

The relation between the spectrometer current in amperes and the magnetic field at the central orbit of 12-in. radius was established by flip coil measurements and is shown in Fig. 4. These data were verified using a Hall probe which in turn was calibrated in a uniform magnetic field standardized using proton resonance. The deviation from linearity was negligible up to about 80 Mev/c. The α particles used have a magnetic rigidity equal to that of an electron of 97.9 Mev/c momentum.

TABLE I. Spectrometer resolution function for channels a, b, and c.

	$G(\xi)$				$G(\xi)$		
ξ	a	b	c	ξ	a	b	c
−0.064	0.000	0.000		+0.002	0.995	0.996	0.994
−0.062	0.001	0.000		0.004	0.978	0.982	0.979
−0.060	0.002	0.000		0.006	0.938	0.949	0.943
				+0.008	0.890	0.905	0.900
−0.058	0.002	0.000					
−0.056	0.004	0.000		+0.010	0.841	0.853	0.853
−0.054	0.005	0.000		0.012	0.790	0.797	0.794
−0.052	0.006	0.000		0.014	0.740	0.739	0.719
−0.050	0.007	0.001	0.000	0.016	0.689	0.678	0.644
				+0.018	0.634	0.610	0.568
−0.048	0.008	0.002	0.000				
−0.046	0.010	0.004	0.000	+0.020	0.579	0.541	0.493
−0.044	0.011	0.006	0.001	0.022	0.518	0.472	0.423
−0.042	0.013	0.008	0.002	0.024	0.454	0.404	0.358
−0.040	0.014	0.012	0.005	0.026	0.390	0.336	0.296
				+0.028	0.342	0.276	0.238
−0.038	0.015	0.016	0.012				
−0.036	0.017	0.025	0.031	+0.030	0.304	0.229	0.187
−0.034	0.028	0.042	0.065	0.032	0.269	0.189	0.147
−0.032	0.057	0.066	0.104	0.034	0.235	0.162	0.114
−0.030	0.097	0.100	0.149	0.036	0.207	0.140	0.082
				+0.038	0.180	0.121	0.061
−0.028	0.142	0.146	0.201				
−0.026	0.193	0.199	0.257	+0.040	0.155	0.102	0.048
−0.024	0.253	0.256	0.313	0.042	0.133	0.084	0.036
−0.022	0.320	0.316	0.371	0.044	0.119	0.068	0.026
−0.020	0.391	0.378	0.434	0.046	0.106	0.056	0.018
				+0.048	0.094	0.045	0.011
−0.018	0.467	0.442	0.501				
−0.016	0.547	0.509	0.572	+0.050	0.082	0.036	0.006
−0.014	0.638	0.580	0.633	0.052	0.071	0.029	0.002
−0.012	0.721	0.656	0.696	0.054	0.060	0.022	0.000
−0.010	0.811	0.739	0.764	0.056	0.050	0.016	
				+0.058	0.040	0.012	
−0.008	0.911	0.816	0.836				
−0.006	0.970	0.888	0.920	+0.060	0.030	0.009	
−0.004	0.991	0.953	0.975	0.062	0.020	0.006	
−0.002	0.999	0.992	0.993	0.064	0.010	0.004	
0.000	1.000	1.000	1.000	+0.066	0.000	0.003	
				+0.068		0.002	

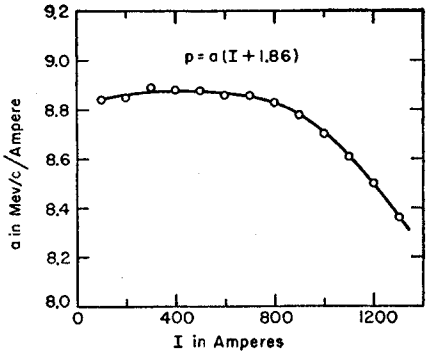

FIG. 4. Magnetic field calibration of spectrometer at 12-in. radius. Ordinates are given in units of momentum in Mev/c divided by current in amperes.

We used this as a fixed point for the momentum calibration of the spectrometer. However, saturation effects are noticeable at this setting so that there is some uncertainty in the absolute value of this point in the calibration.

ARRANGEMENT

The positive pions from this experiment were obtained from the Chicago Synchrocyclotron. By extracting the pions from an internal target through an evacuated pipe connected directly to the cyclotron vacuum chamber it was possible to obtain improved focussing and energy homogeneity in the beam. The beam used had an energy of 62.9 Mev as determined by range measurements in polyethylene. The manner of introducing the pions into the spectrometer is shown in Fig. 5. Pions were focussed by a wedge magnet (not shown) and enter the spectrometer by traversing counters 1 and 2. They were moderated in polyethylene so that, for the most part, they came to rest in the source counter 3. Electrons emerging from counter 3 with the proper energy and direction were focussed to traverse one of the counters 4a, 4b, or 4c, and counter 5. Counter 1 was a reduced area counter used to check on the counting losses in counter 2. Counter 3 was a block of plastic scintillator (Pilot B) 1.5 in.×2.83 in.×0.5 in. set at 45° with respect to the pion beam. The scintillator block was supported by a hollow square tube aluminized on the inside for light piping. Transition to a Lucite light pipe was made $5\frac{3}{4}$ in. behind the scintillator. This arrangement minimized the amount of material in the vicinity of the scintillator in which pions could stop and yet give a measurable electron pulse. Details of the arrangement are given in Fig. 6.

The electronic circuits were designed so that events which had a time dependence appropriate to the π-e decay process would be recorded with a travelling wave oscilloscope. For each selected event the pulses appearing on counters 3 and 5 were displayed on the oscilloscope screen and photographed. Thus, each event could be studied at leisure, the significant time re-

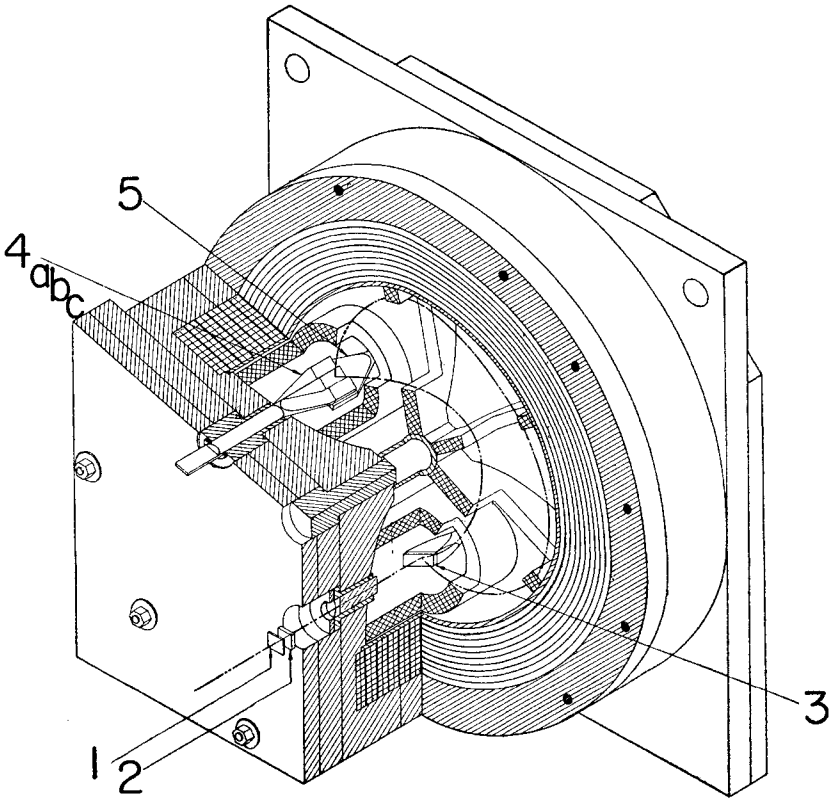

FIG. 5. Perspective view of spectrometer. The counters are indicated by number.

lationships and pulse heights accurately measured, and spurious events identified.

A block diagram of the electronics is given in Fig. 7. Pions traversing counter 2 and reaching counter 3 produced a coincidence (23). An electron emerging from counter 3 and reaching counter 5 produced a coincidence (35). The coincidence $(\overline{23})$ (35) 4*a*, identifying an electron in channel *a*, produced a pulse of 200 mμsec duration. The use of an anticoincidence $(\overline{23})$ here ruled out accidentals between pions triggering (23) and spurious count in 4*a*, 5. The final coincidence was formed between the delayed (23) pion pulse and the 200 mμsec output pulse of $(\overline{23})$ (35) 4*a*. When an electron appeared in the 200 mμsec interval starting 17 mμsec after the arrival of the pion in counter 3, this operated a bi-stable flip-flop which triggered the travelling wave oscilloscope. The same circuit stopped the count, indicating by a signal light that it had done so. Triplicate circuitry was provided so that observations in the 3 adjacent channels, *a*, *b*, and *c*, could be recorded simultaneously. The circuits used newly available high speed diodes and transistors and were designed along lines described by one of us (RHM).[14] A more detailed description of the circuits used here will be given elsewhere.

Each triggered event was photographed on 35 mm Agfa Isopan Record film by means of an $F/0.7$ camera. Film was advanced and the circuit reset by hand after each event. Timing diagrams in Fig. 7 illustrate the time sequence of pulses in a π-e event for two different time delays in the emission of the electron. The pulses were produced in RCA-7264 14 stage photomultiplier tubes which viewed the scintillation counters through Lucite light pipes. The pulses were clipped by $1\frac{1}{2}$ feet of RG 62/U terminated in 39 ohms and delivered through 350 feet of Styroflex 100-ohm cable directly to the deflection plates of the oscilloscope tube. The clipping line was carefully designed to make the counter pulse as short as possible without excessive loss of pulse height, and to avoid overshoot on the trailing edge of the pulse. Using a light pulser which was modified to produce two light pulses 12 mμsec apart, we verified that this clipping arrangement would permit the small electron pulse to be clearly seen at short times after the pion pulse. The output of counter 3 was connected to the upper helix of the oscilloscope to give positive deflections on the film while that from counter 5, delayed by an additional 25 feet was connected to the lower helix to give negative deflections. No amplification was used and careful attention was given to the matching of impedance to assure faithful reproduction of the pulses. The photomultiplier tubes were carefully shielded against stray magnetic fields and it was demonstrated that the pulse height recorded was not affected by the current setting of the spectrometer.

[14] R. H. Miller, Rev. Sci. Instr. **30**, 395 (1959).

OBSERVATIONS

The signature of a π-e event appeared on the film as a large positive pulse due to a stopping pion in counter 3, a smaller second pulse due to an electron leaving counter 3, followed by a small negative pulse due to the electron arriving at counter 5. The delays fixed the timing between the final $(+, -)$ pair to be 34 mμsec. The time between the two positive pulses was the time for which that particular pion lived. Typical photographs of the π-e events recorded with the spectrometer set at 760 amperes are shown in Fig. 8. Calibration of the oscilloscope sweep and correction for its nonlinearity were established by a 100-megacycle signal at frequent intervals throughout the run.

Lower current settings of the spectrometer were used to record π-μ-e events. The muon causes an additional positive pulse to appear between the pion and the final $(+, -)$ pair. However, when the π-μ timing was less than 14 mμsec the two pulses were not always clearly resolved. Such events occurred about as often as those in which the μ pulse was clearly resolved. Examples of π-μ-e events taken at 450 amperes (40 Mev/c) are shown in Fig. 9. Only a small fraction (5%) of the μ electrons which reached the detector were early enough to trigger the oscilloscope. This was because the coincidence circuits accepted only those arriving less than 220 mμsec after the pion pulse. Accidental coincidences between an electron and an unrelated pion were appreciable at full beam intensity. For this reason the photographs of the π-μ-e events were made at lowered beam intensity. An estimate of the accidental rate was made by removing the delay in the output of (2,3) and photographing the triggered events so obtained for various beam intensities. In this case the triggers were accidental coincidence caused by electrons in (3,4,5) which came earlier than the pions in (2,3). Figure 10 shows how the rate of these accidentals varies with beam intensity. At the intensity used for photographing the π-μ-e events at 450 amperes, 3% of the events were accidentals.

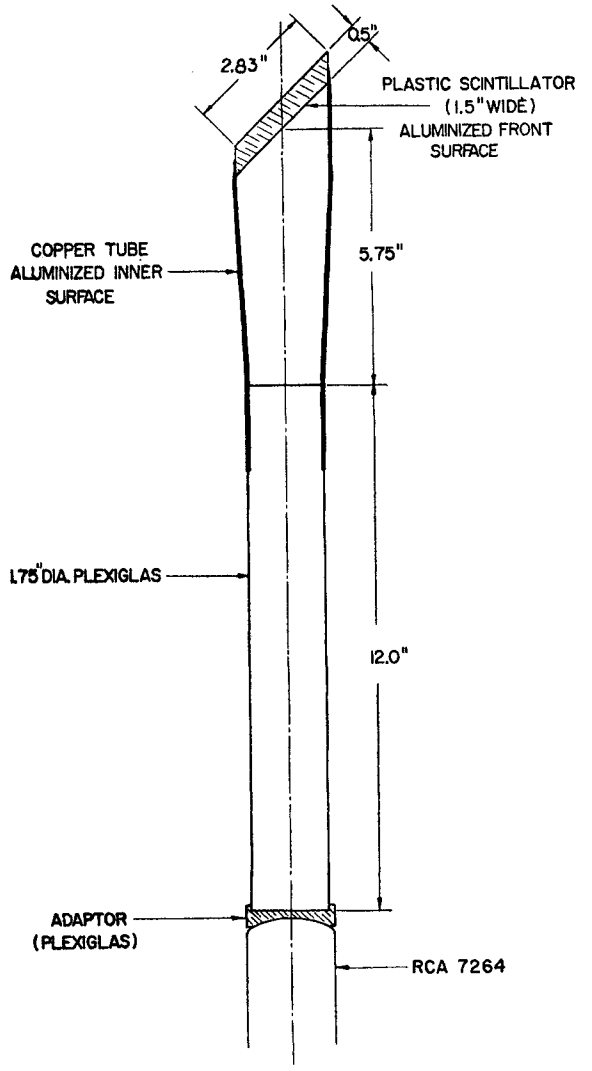

FIG. 6. Detail of counter 3, showing the composite construction of the light pipe. Light conduction is by aluminized reflector followed by a Lucite light pipe.

SPURIOUS EVENTS

Among the traces which appeared to have the correct π-e signature were some which were caused by spurious processes. We relied on the timing t_{35} between the electron pulses in counters 3 and 5 to help distinguish one kind of false π-e event. Figure 11 shows the t_{35} timing as observed for 729 π-μ-e events taken at 450 amperes. In all but 3 events the t_{35} timing lies within the interval 31 to 37 mμsec so that this interval was taken to identify an electron in the spectrometer. Most of the dispersion in the timing was due to differences in the flight path of the electrons in traversing different trajectories in the spectrometer. In the same figure the t_{35} timing for π-e events obtained at the high current settings of the spectrometer is plotted. Out of 1488 events 1346 had the correct t_{35} timing. The remaining 142 events were considered to be spurious and were not included in the final tally.

A study of the pulse-height distribution of these rejected events indicated that many of them may have been produced by muons in counter 3 in accidental coincidence with a pair of pulses in counters 4 and 5 such as might have been produced by a stray electron or other cause. The correct timing between a pion produced coincidence in (2,3) and the succeeding positive pulse from counter 3 is provided by the ordinary π-μ decay, while the remaining negative pulse from counter 5 could appear with approximately the correct timing by accident. In Fig. 12 the counter 3 "electron" pulses for the rejected events are compared with those from the accepted events. Many of the rejected events have the 1.3-mm pulse-height char-

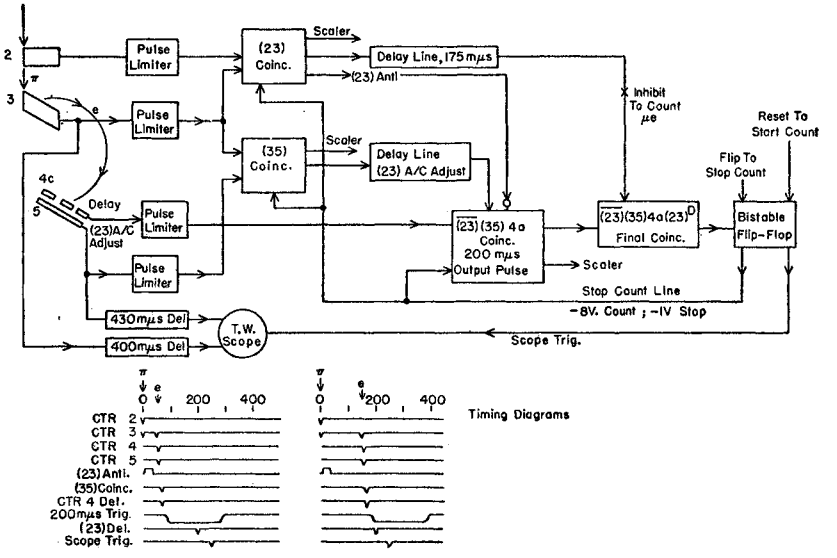

FIG. 7. Block diagram of the electronics. Typical timing sequences are shown.

acteristic of muons (see Fig. 17). The second positive pulse from counter 3 might also have been caused by another pion or by an electron not genetically related to the pion responsible for the (2,3) coincidence. The smaller and larger pulses which appear among the rejected events of Fig. 12 are presumably due to such causes. False events of this type with timing t_{35} inside the 6 mμsec wide acceptance interval, should occur as frequently as those outside in an interval equally wide. Accordingly, we adopted the rule that whenever a false π-e event was found in a given channel at a given current with timing t_{35} in the interval 28–31 mμsec or 37–40 mμsec, we subtracted one event from the tally of accepted events for that current and channel. Thus, we wrote

$$[\pi e]_{\text{net}}=[\pi e]_{\text{accepted}}-[\pi e]_{\text{rejected}}.$$

In all, we subtracted 80 events by this procedure.

The number of events $[\pi e]_{\text{net}}$ obtained in this way still includes another type of spurious event. Events of this type could be obtained by π-μ-e processes in which the μ electron, by scattering, produces correctly timed pulses in counters 3, 4, and 5, and in which the μ pulse comes too early to be clearly distinguishable from the π pulse. The measurements at 450 amperes showed, however, that when actual π-μ-e processes are observed, events with the μ appearing later than 14 mμsec occur as often as those with an earlier μ. These events without a distinguishable μ pulse would be classified as π-e events at the higher currents. To remove such events from the tally we used the rule that whenever a π-μ-e event was found at a given current in a given channel, with the μ pulse later than 14 mμsec, we subtracted one from the number $[\pi e]_{\text{net}}$ for that current and channel. However, all events of the type $\pi(+)e$ [see Fig. 8(b)] might not be due to a π-μ-e process. These could be true π-e events with an extra positive pulse superimposed by accident. But if such events could be caused accidentally, the same cause would also produce events with an extra positive pulse appearing *after* the e_3 pulse. These are denoted $\pi e(+)$ [see Fig. 8(c)]. From the timing relations we deduced that the probability of finding a $\pi(+)e$ event was 0.7 times that for a $\pi e(+)$ event. Thus, we obtained the number of $\pi\mu e$ events using the rule

$$[\pi\mu e]=[\pi(+)e]_{\text{accepted}}-0.7[\pi e(+)]_{\text{accepted}},$$

and the true number of π-e events was obtained using the rule

$$[\pi e]_{\text{true}}=[\pi e]_{\text{net}}-[\pi\mu e].$$

PION LIFETIME

To verify that the observed events had the time behavior pion decay we prepared a tally of the times $t_{\pi e}$ between pion and electron pulse in counter 3. We used only clear π-e events and did not include those in which an extra positive pulse appeared, such as $\pi(+)e$ and $\pi e(+)$. No correction was made for spurious events of the type $\pi\mu$ + accidental (4,5) as discussed above because the time between the first two positive pulses would in this case still be characterized by the π lifetime. On the other hand, spurious events due to scattered μ electrons would have the wrong time behavior and for this reason a correction for the fraction of these to be expected in each time interval was made. The mean life was calculated from the tally of times using the following formula:

$$\tau_\pi=\frac{\sum_{i=1}^{N}(t_{\pi e})_i}{N(1-f_\mu)}-\frac{f_\mu}{1-f_\mu}\left(\frac{T_1+T_2}{2}\right)-T_1+\frac{T_2-T_1}{e^{(T_2-T_1)/\tau_\pi}-1},$$

Here, N is the total number of events (973); $f_\mu=[\pi\mu e]/[\pi e]_{\text{accepted}}$ is the fraction of events due to scattered μ electrons; T_2 (=150 mμsec) is the upper limit of the time $t_{\pi e}$ of accepted events; T_1 is the lower limit. The

coincidence circuits permit different cutoff times T_1 for each channel. This time was determined from the data to be 20, 28, and 24 mμsec for channels *a*, *b*, and *c*, respectively. No significant effect on the results was found upon increasing T_1 by 3 mμsec. The first term is the sum of all times divided by the number of π-*e* events; the second term corrects for the μ-*e* events present; the third term corrects for the events which came earlier than T_1; the last term corrects for the events coming after T_2. We obtained $\tau_\pi = 25.3 \pm 0.9$ mμsec. The data are plotted as a differential decay curve in Fig. 13 and shows a good agreement with this

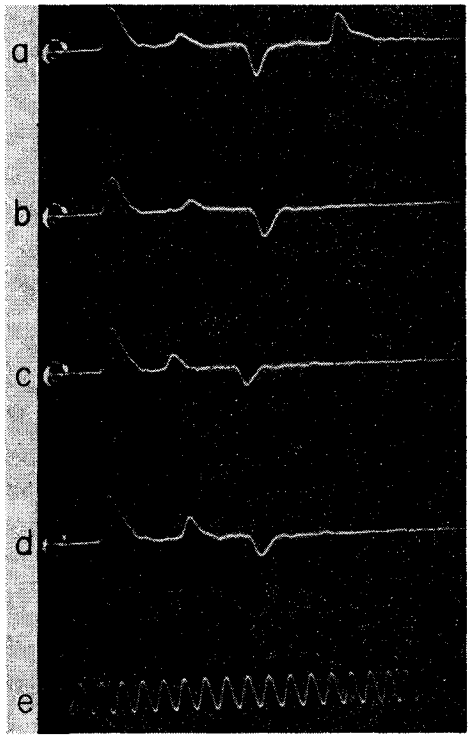

(a)

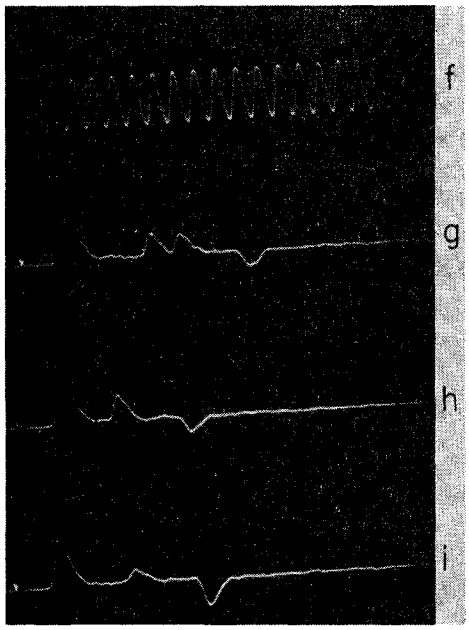

(b)

FIG. 8. Photographs of π-*e* events taken at 760 amperes. Traces *b*, *c*, *d*, *h*, and *i* are normal πe events; an event of type $\pi e(+)$ is shown in *a* and of type $\pi(+)e$ in *g*. The 100-megacycle timing wave is shown in *e* and *f*.

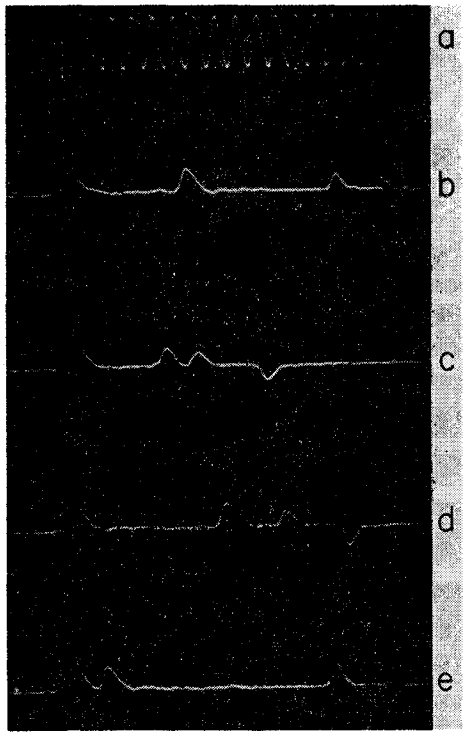

FIG. 9. Photographs of π-μ-*e* events taken at 450 amperes. The 100-megacycle timing wave is shown in *a*.

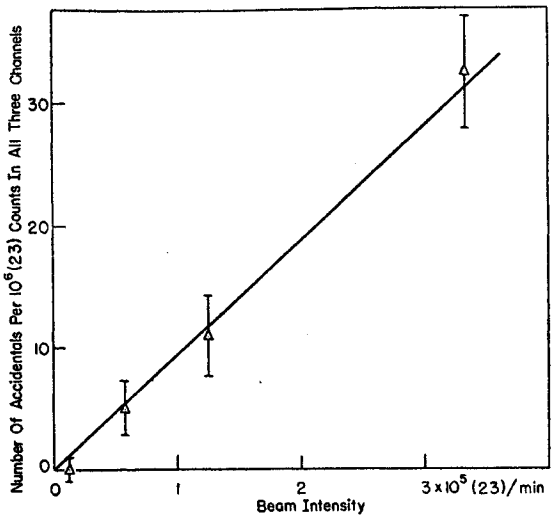

FIG. 10. Accidentals in recording π-μ-*e* events at 450 amperes.

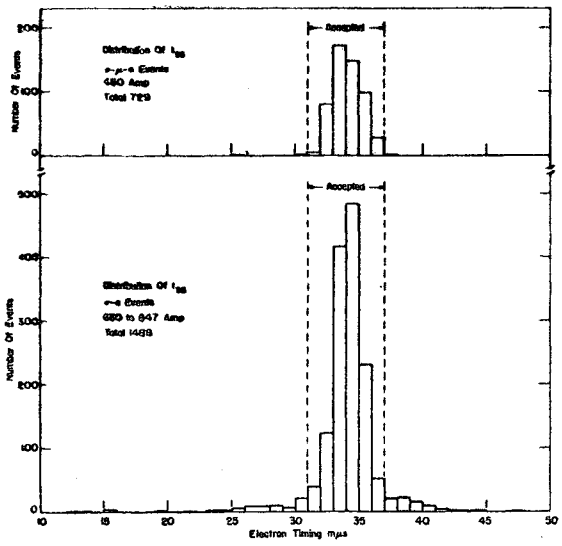

FIG. 11. Timing t_{35} between electron pulses in counters 3 and 5 for π-μ-e events at 450 amperes and for π-e events in the range between 630 and 847 amperes. The ordinates specify number of events per mμsec.

value of the mean life. The points earlier than 30 mμsec fall lower than the curve because of the action of the anticoincidence circuit. This result may be compared with the lifetime as determined from the timing $t_{\pi\mu}$ in the π-μ-e events obtained at 450 amperes. The data are plotted in Fig. 14 and compared with the curve obtained as the best fit by a least squares criterion. This gave for the lifetime $\tau_\pi = 26.3 \pm 1.4$ mμsec. The curvature shown in the figure appears because only those π-μ decays were recorded in which the electron appeared less than 150 mμsec after the π. Late appearing μ's have a reduced chance of decaying within the smaller time interval remaining.

The values of the pion lifetime obtained from these two sets of observations are in good agreement with one another. The weighted average of the two measurements gives $\tau_\pi = 25.6 \pm 0.8$ mμsec. This has comparable accuracy and is in good agreement with other measurements.

The time distribution $t_{\pi e}$ of π-μ-e events can be expected to differ markedly from that of π-e events. This is evident in the plot of Fig. 15 taken from the 450 ampere data. A comparison with the calculated curve is shown. Again, the points earlier than 30 mμsec fall below the curve because of the action of the anticoincidence ($\overline{23}$).

The over-all conformity of the timing measurements with the known characteristics of the π and μ decay gives us confidence in the validity of the analysis.

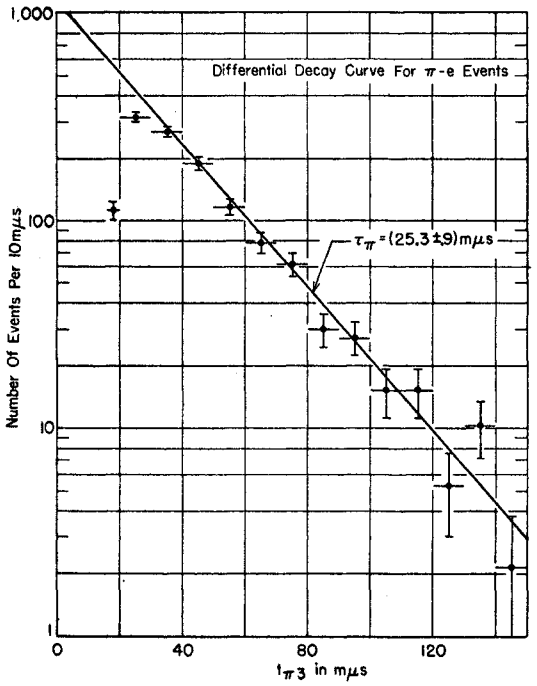

FIG. 13. Differential decay curve for π-e events. The first two points fall below the calculated curve because of the action of the anticoincidence.

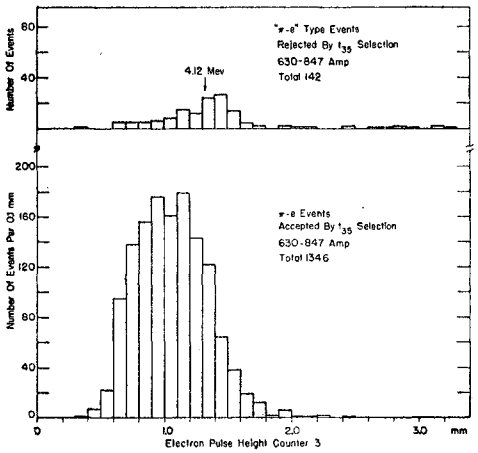

FIG. 12. Pulse-height distribution of accepted and rejected π-e events.

ANALYSIS

A compilation of the π-e events found in each channel at each of the current settings used, together with the corresponding total number of monitor counts, is given in Table II. The contribution of the occasional event which registered in more than one channel was divided equally among them. The spectrum of μ electrons was obtained by counting ($\overline{23}$) (35) (4) coincidences with the (23) delayed coincidence condition removed. With this arrangement all μ electrons were counted except those which came so early that the anticoincidence action excluded them. These data are collected in Table III. In Fig. 16 both the π-e and the μ-e data appear plotted together. In this plot the data from channels a and c have been normalized to give the same

total number of electrons as channel *b*. The same normalization factors were applied to the π-e data which are, however, exhibited on an expanded scale. Moreover, a correction for decay was made to take into account the events missed because they fell outside the interval of acceptance of the circuit. Thus, all the π-e and all the μ-e data were placed on a comparable basis. The two distributions appear nicely separated, and the branching ratio can be determined from a comparison of the number of electrons in each of them.

In view of the limited statistics at each point, there was some question how best to determine the area under the π-e distribution. This was especially difficult because of the long tail produced below the π-e peak by the effect of radiative processes. The problem was solved by taking into account the known properties of the spectrometer and the known causes of spectrum distortion to infer the expected shape of the curve and then fitting the data by a least squares procedure. This verified the consistency of the data with what could be expected and provided a basis for estimating the errors.

The π-e spectrum is a delta function, modified by internal radiative effects. To the extent that they can influence the observations, these effects can be accounted for by adding a small second term to the distribution writing,

$$Q(\eta)d\eta=\alpha\delta(\eta)d\eta+\beta(d\eta/\eta), \qquad (1)$$

where $\eta=E_\pi-E$ measure the difference between the electron energy[15] E and its maximum possible value, $E_\pi=\frac{1}{2}m_\pi=69.8$ Mev. The second term is limited to apply only within the range between a lower bound η_1, chosen small compared to the resolution width of the spectrometer, and an upper bound η_2 chosen large compared to the same quantity, but small compared to E_π. With these restrictions the constants α and β are chosen such that $\int Q(\eta)d\eta=1$. This neglects radiative effects for which $\eta<\eta_1$ by lumping such electrons in the delta function part. Electrons with $\eta>\eta_2$ are not included in the reduction of the data but are accounted for in the final value of the branching ratio. It is not possible to distinguish the radiative part from that not so affected in the present experiment. Accordingly, we have relied on Berman's calculations[6] in determining the relative importance of the two terms. These show that if we choose $\eta_1=0.3$ Mev and $\eta_2=10.0$ Mev, as is appropriate in the present case, then 7.7% of the electrons are accounted for by the second term and the remainder, 92.3%, by the first term.

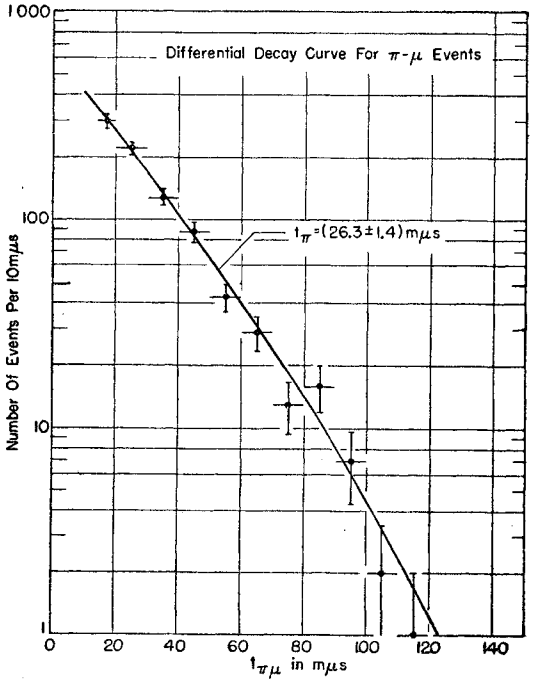

FIG. 14. Differential decay curve for π-μ events. The calculated curve departs from a straight line because of the action of the gate.

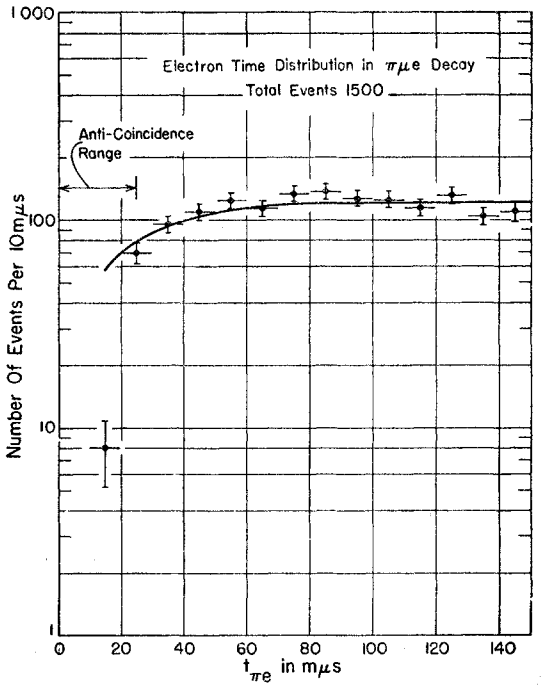

FIG. 15. Electron time distribution in π-μ-e events at 450 amperes.

IONIZATION LOSS

The ionization loss in the source broadens the original distribution primarily because the electrons originate in different depths within the source. The fluctuations

[15] The electron energies referred to in this paper are always total energies (including rest mass). These have numerical values differing inappreciably from the corresponding momenta over the range covered in this experiment. Thus, invariant functions of the momentum may be taken to be invariant functions of the total energy as well.

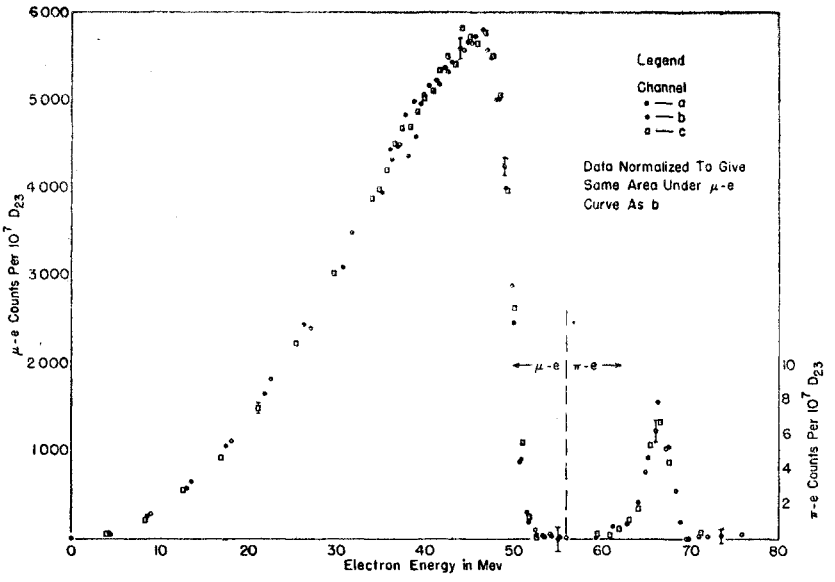

FIG. 16. Combined plot of π-e and μ-e data. Note the change in scale above 55 Mev. Errors are indicated at selected points.

in the ionization loss (Landau effect) produce a further broadening. A useful measure of the combined effect may be obtained from the heights of the pulses produced by the electrons in counter 3. We used the pulse-height distribution obtained with μ electrons at 450 amperes (40 Mev/c in channel b). This made it possible to record losses up to about 13 Mev, the maximum allowed because of the cutoff in the μ-e spectrum. It served our purpose because the ionization loss for electrons at this energy is virtually the same as for other energies within the range encompassed in this experiment. To the extent that the energy spectrum is flat the spectrometer will sample uniformly the distribution in the pulse heights which is present. As a matter of fact, the energy spectrum has a positive slope at this setting and a small correction was applied to account for the bias by the spectrometer in favor of electrons with a somewhat higher energy loss.

TABLE II Compilation of π-e events.

Amp.	Channel	Mev	Monitor $D_{23}\times10^{-7}$	$[\pi e]$ accept.	$[\pi e]$ rej.	$[\pi e]$ net	$[\pi(+)e]$ accept.	$[\pi e(+)]$ accept.	$[\pi e]$ true	$[\pi e]$ true/$(D_{23}\times10^{-7})$
630	a	56.87	6.193	2.0	1.0	1.0	1.0	0.0	0.0	0.00±0.32
	b	55.17		1.0	0.0	1.0	1.0	0.0	0.0	0.00±0.23
	c	53.88		4.0	1.0	3.0	7.0	0.0	−4.0	−0.65±0.56
679	a	61.25	14.552	5.5	0.0	5.5	1.0	0.0	4.5	0.31±0.18
	b	59.42		1.5	0.0	1.5	1.0	0.0	0.5	0.03±0.11
	c	57.49		6.0	2.0	4.0	2.0	0.0	2.0	0.14±0.22
720	a	64.88	25.907	47.0	3.0	44.0	3.0	1.0	41.7	1.61±0.28
	b	62.94		10.5	1.0	9.5	2.0	0.0	7.5	0.29±0.14
	c	60.90		7.5	3.0	4.5	2.0	0.0	2.5	0.10±0.14
734	a	66.09	40.964	106.5	1.0	105.5	1.0	2.0	105.9	2.59±0.26
	b	64.11		31.5	2.0	29.5	2.0	1.0	28.2	0.69±0.15
	c	62.04		15.0	2.0	13.0	2.0	0.0	11.0	0.27±0.11
747	a	67.23	41.107	95.5	5.0	90.5	3.0	2.0	88.9	2.16±0.25
	b	65.23		66.0	3.0	63.0	1.0	2.0	63.4	1.53±0.21
	c	63.11		25.5	2.0	23.5	3.0	0.0	20.5	0.50±0.13
760	a	68.37	67.483	82.0	2.5	79.5	2.0	1.0	78.2	1.16±0.14
	b	66.32		184.0	6.5	177.5	6.5	4.0	173.8	2.57±0.21
	c	64.18		65.0	7.0	58.0	5.5	3.0	54.6	0.81±0.14
775	a	69.69	42.207	6.0	5.0	1.0	1.0	0.0	0.0	0.00±0.08
	b	67.60		79.5	6.0	73.5	2.0	2.0	72.9	1.73±0.22
	c	65.41		113.5	3.0	110.5	8.0	2.0	103.9	2.46±0.27
790	a	71.00	39.242	7.5	4.5	3.0	1.0	0.0	2.0	0.05±0.09
	b	68.87		15.5	2.0	13.5	1.0	0.0	12.5	0.32±0.11
	c	66.63		126.0	3.5	122.5	5.0	2.0	118.9	3.03±0.30
802	a	72.04	28.314	6.0	2.0	4.0	2.0	0.0	2.0	0.07±0.11
	b	69.88		7.0	3.0	4.0	4.0	0.0	0.0	0.00±0.13
	c	67.72		63.0	6.0	57.0	2.0	3.0	57.1	2.01±0.30
847	a	75.91	16.325	4.0	2.0	2.0	1.0	1.0	1.7	0.10±0.17
	b	73.64		2.5	0.5	2.0	1.0	0.0	1.0	0.06±0.12
	c	71.24		4.5	0.5	4.0	1.0	0.0	3.0	0.18±0.16

The calibration of the pulse height in Mev was obtained with pions. The CH_2 moderator was removed and the full energy pions (63 Mev) were allowed to traverse the scintillator of counter 3. The mean pulse height was found to be 1.85 mm; the actual distribution being given in Fig. 17. We used the fact that 63-Mev pions traversing 1.89 g/cm² of polystyrene lose 5.51 Mev, to conclude that the mean ionization loss must be 3.0 Mev/mm. The muons associated with the π-μ-e events observed here also give a pulse-height distribution which was used as a check on the calibration. This distribution is also shown in Fig. 17. The mean pulse height is 1.32 mm and is due to an energy loss of 4.12 Mev by the muons. Saturation effects in the scintillator affect this calibration, but it is, nevertheless, in good agreement with the result obtained with the pions.

Some broadening in the observed distribution is due to the fluctuations in the response of the photomultiplier because of the finite number of light quanta collected. This was the principal cause of the width observed in the muon pulse-height data, from which it could be shown that this effect could have only a minor influence on the observed distribution with electrons. Nevertheless, it was corrected for by carrying out an unfolding procedure which gave the function $\mathcal{L}(\epsilon)$ tabulated in Table IV. This gives the energy loss by ionization of the electrons in the source. It is normalized so that $\sum \mathcal{L}(\epsilon)\Delta\epsilon = 1$.

TABLE III. Measured μ-e spectrum: The errors are based on counting statistics only. No background count has been subtracted.

Current in amp	Counts per 10^6 D_{23} Channel a	Channel b	Channel c
0	0.3± 0.3	0.3± 0.3	0.0± 0.3
50	4.7± 1.1	5.6± 1.2	6.4± 1.3
100	25.9± 2.7	26.1± 2.7	25.0± 2.6
150	61.4± 4.1	57.0± 4.0	64.7± 4.2
200	103.1± 5.3	104.8± 5.3	108.0± 5.4
250	169.5± 6.8	164.3± 6.7	173.9± 6.9
300	223.1± 7.8	242.9± 8.1	262.2± 8.4
350	323.8± 9.4	308.0± 9.1	355.7± 9.8
400	402.2±10.4	394.3±10.3	454.9±11.1
410	417.5±12.3	443.7±12.7	468.7±13.0
420	406.5±12.1	446.8±12.7	494.0±13.4
430	427.3±12.5	482.6±13.2	529.8±13.8
440	470.7±13.0	498.9±13.4	550.7±14.1
450	477.7±11.3	495.2±11.5	552.4±12.2
460	482.2±11.4	516.4±11.8	572.0±12.4
470	495.3±11.5	522.2±11.9	590.8±12.6
480	500.1±11.6	536.9±12.0	598.9±12.7
490	517.8±11.8	542.8±12.1	627.5±13.0
500	524.6±11.8	558.6±12.2	647.1±13.2
510	522.8±11.8	566.2±12.3	635.8±13.0
520	511.4±11.7	572.9±12.4	684.8±13.6
530	466.1±11.1	580.0±12.5	674.0±13.4
540	396.5±10.3	547.3±12.1	663.6±13.3
550	268.2± 8.5	501.2±11.5	678.5±13.4
560	118.1± 5.6	399.0±10.3	648.1±13.1
570	28.3± 2.8	245.5± 8.1	594.7±12.6
580	5.3± 1.2	90.4± 4.9	467.9±11.2
590	3.2± 0.9	18.9± 2.2	309.4± 9.1
600	3.5± 1.0	4.5± 1.1	128.4± 5.8
610	1.9± 0.7	2.4± 0.8	29.8± 2.8
620	1.1± 0.5	3.5± 1.0	4.2± 1.1

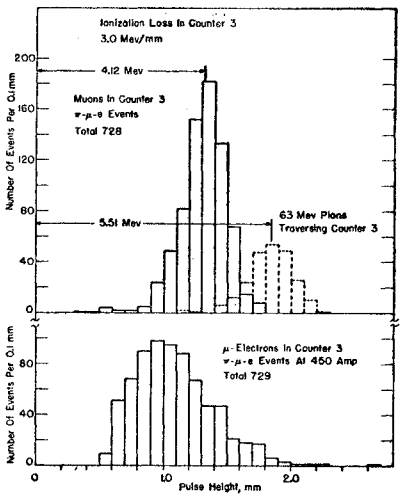

FIG. 17. Calibration of ionization loss. Upper figure gives the pulse-height distribution of 63-Mev pions and also of the muons from stopped pions. Lower figure gives the pulse-height distribution of the μ electrons at 450 amperes.

BREMSSTRAHLUNG LOSS

To correct for the effect of external bremsstrahlung on the shape of the observed distribution, we used the function $\mathcal{L}(\epsilon)$ as a measure of the thickness of source traversed. Thus, an electron losing an amount of energy ϵ by ionization, would lose an additional amount proportional to ϵ with a probability calculable by means of the Bethe-Heitler formula.[16] For scintillator material (polystyrene) the average ionization loss was taken to be[17] 2.00 Mev/g/cm². For our case (complete screening approximation) the formula reduces to

$$B(E,K)dK = 1.514\times10^{-2}\epsilon\left(1-\frac{K}{E}+0.7376\frac{K^2}{E^2}\right)\frac{dK}{K} = \epsilon F(E,K)dK, \quad (2)$$

where E is the initial energy of the electron, K its loss by bremsstrahlung, and ϵ its loss by ionization in Mev.

To simplify the calculation, we supposed that all the ionization loss occurs after the bremsstrahlung takes place. Thus, an electron may leave the source with a total energy loss ζ by losing an energy ϵ by ionization and the remainder $\zeta-\epsilon$ by bremsstrahlung. Electrons

[16] E. Segrè, *Experimental Nuclear Physics* (John Wiley & Sons, Inc., New York, 1953), Vol. I, Part II, p. 260.

[17] We used the results given in the paper of R. M. Sternheimer, Phys. Rev. **103**, 511 (1956) and took into account the fact that our electrons are positive and therefore ionize less. See B. Rossi, *High-Energy Particles* (Prentice-Hall, Inc., New York, 1952), Chap. 2, p. 27. It would have been more correct to take an even smaller value because the large energy losses (above 10 Mev) are included in the average but not in our ionization loss function $\mathcal{L}(\epsilon)$. The adjustment this calls for in the final result will be discussed later.

TABLE IV. Energy loss function (normalized to $\Sigma\mathfrak{L}(\epsilon)\Delta\epsilon=1$).

Energy loss ϵ (Mev)	$\mathfrak{L}(\epsilon)$
0 –1.5	0.000
1.5–1.8	0.042
1.8–2.1	0.238
2.1–2.4	0.316
2.4–2.7	0.417
2.7–3.0	0.451
3.0–3.3	0.436
3.3–3.6	0.402
3.6–3.9	0.304
3.9–4.2	0.213
4.2–4.5	0.212
4.5–4.8	0.094
4.8–5.1	0.080
5.1–5.4	0.075
5.4–5.7	0.027
5.7–6.0	0.013
6.0–6.3	0.004
6.3–6.6	0.004
6.6–6.9	0.004
6.9–∞	0.000

with an initial energy E will have a total energy loss distribution given by[18]

$$M(E,\xi)=\int \epsilon\mathfrak{L}(\epsilon)F(E,\xi-\epsilon)d\epsilon \tag{3}$$

Using this the modified energy distribution of the π electrons is obtained from (1) to be

$$S(E')=\int M(E,E'-E)Q(E)dE. \tag{4}$$

The numerical work was carried out with desk calculators and was somewhat simplified to reduce the labor without much loss in the accuracy. Thus, the correction for external bremsstrahlung was applied only to the delta function part of the initial spectrum. That is, radiative effects, whether internal or external, were taken to operate only once; multiple radiative effects were neglected. To the extent that it is permissible to neglect such processes as annihilation in flight, Bhabha scattering and pair production, which do not conserve the number of electrons, it follows from the normalizations already adopted that also $\int S(E')dE'\cong 1$.

BRANCHING RATIO

The expected response of the spectrometer when it is set at energy E_0 will be proportional to the overlap function,

$$\mathcal{O}(E_0)=\int S(E')G\left(\frac{E'-E_0}{E_0}\right)dE'. \tag{5}$$

Here, $G((E'-E_0)/E_0)$ is the resolution function of the spectrometer. It is very nearly independent of E_0 over the range of energies of importance here and is taken to be the same function $G(\xi)$ determined by the α-particle calibration. Small deviations in the behavior of this function may be introduced by the effect of scattering at the slits and baffles of the spectrometer, but can have only a minor influence on the final result.

The counting rate for the π electrons may be written

$$N_\pi(E_0)=fC_\pi\mathcal{O}_\pi(E_0) \tag{6}$$

where f is the branching ratio to be determined and C_π is the factor of proportionality which summarizes the purely experimental factors entering into the observation of the π electrons. The corresponding counting rate for the μ electrons is written,

$$N_\mu(E_0)=C_\mu\mathcal{O}_\mu(E_0). \tag{7}$$

The branching ratio which is obtained by integrating over the observed distributions is insensitive to a detailed knowledge of any of the functions that enter into the overlap integral $\mathcal{O}(E_0)$. Consider the integral,

$$J=\int\frac{N(E_0)dE_0}{E_0}, \tag{8}$$

and note that

$$\frac{dE_0}{E_0}=-\frac{d\xi}{1+\xi} \quad \text{with} \quad \xi=\frac{E'-E_0}{E_0}.$$

Then,

$$J_\pi=fC_\pi\int G(\xi)\frac{d\xi}{1+\xi}, \tag{9}$$

and

$$J_\mu=C_\mu\int G(\xi)\frac{d\xi}{1+\xi}, \tag{10}$$

so that the branching ratio is given by,

$$f=\frac{J_\pi}{J_\mu}\frac{C_\mu}{C_\pi}. \tag{11}$$

We obtained J_π from a least squares fit to the data in the region well above the μ-e end point using the formula

$$N_\pi(E_0)=J_\pi\frac{\mathcal{O}_\pi(E_0)}{\int\mathcal{O}_\pi(E_0)dE_0/E_0}. \tag{12}$$

For the μ electrons the observations were extended over the whole spectrum so that it was sufficient to integrate the experimental points directly to obtain J_μ. Since energy is very nearly proportional to current in the spectrometer over the range covered by the μ-e spectrum we simply calculated the integral,

$$J_\mu=\int N_\mu(I)\frac{dI}{I}, \tag{13}$$

[18] Where limits are not explicitly given, integrals are intended to be taken over the whole range where the integrand is nonzero.

TABLE V. Summary of branching ratio calculations. Case (A): The π-e spectrum is taken as a delta function and only the ionization loss is taken into account. Case (B): The same as (A) but external bremsstrahlung taken into account. Case (C): The same as (B) but including the extra data obtained when the earlier cut off time T_1 is extended 3 mμsec earlier. Case (D): The same as (C) but including internal radiative effect. The expectation value χ^2 should be near 6 for the individual channels and near 22 for the over-all fit.

Case	Channel	J_π	k	χ^2	Branching ratio $f\times10^4$ Normalized to μ-e pictures	Normalized to μ-e integral
(A)	a	0.1291±0.0084	0.9850	4.33	1.012 ±0.082	0.884 ±0.058
	b	0.1125±0.0071	0.9871	4.52	0.974 ±0.083	0.982 ±0.062
	c	0.1357±0.0089	0.9890	7.36	0.839 ±0.066	0.858 ±0.057
(B)	a	0.1552±0.0098	0.9848	2.76	1.216 ±0.097	1.062 ±0.067
	b	0.1327±0.0083	0.9852	6.38	1.150 ±0.089	1.158 ±0.073
	c	0.1615±0.0104	0.9855	3.81	0.998 ±0.077	1.022 ±0.067
		Weighted mean $\bar{f}$			1.107 ±0.050	1.079 ±0.040
		Weighted mean $\bar{k}$			0.9849±0.0009	0.9852±0.0009
		Total χ^2			16.4	14.9
(C)	a	0.1779±0.0106	0.9853	4.38	1.232 ±0.094	1.082 ±0.065
	b	0.1497±0.0087	0.9861	5.15	1.162 ±0.085	1.161 ±0.068
	c	0.1886±0.0111	0.9854	5.02	1.029 ±0.075	1.060 ±0.063
		Weighted mean $\bar{f}$			1.126 ±0.048	1.099 ±0.038
		Weighted mean $\bar{k}$			0.9854±0.0008	0.9857±0.0008
		Total χ^2			18.0	16.1
(D)	a	0.1879±0.0113	0.9854	4.27	1.301 ±0.100	1.142 ±0.068
	b	0.1569±0.0091	0.9859	5.89	1.217 ±0.090	1.217 ±0.071
	c	0.1972±0.0116	0.9851	5.68	1.076 ±0.078	1.109 ±0.066
		Weighted mean $\bar{f}$			1.178 ±0.051	1.152 ±0.039
		Weighted mean $\bar{k}$			0.9852±0.0009	0.9856±0.0009
		Total χ^2			19.6	17.3

where $N_\mu(I)$ is the count given in Table III for 10^7 monitor counts.

CALCULATIONS

The setting of the spectrometer is known only approximately from the α-particle calibration and the magnetic field measurements. We denote by W the nominal energy at which the spectrometer is set. This differs from the correct energy E_0 by a factor k near unity such that $E_0=kW$. Accordingly, two parameters J_π and k were adjusted to obtain the best fit to the observations according to the χ^2 minimum criterion.

It appeared useful to obtain the best fit values of J_π and k under a series of assumptions of increasing completeness. In every case the calculations were carried out separately for channels a, b, and c. The following cases were considered with results as summarized in Table V:

(A) The π-e spectrum is a delta function and only the ionization loss is taken into account. The data taken for this analysis were those for which T_1 was taken to be 23, 31, and 27 mμsec for channels a, b, and c, respectively (Data I).

(B) The same as (A) but external bremsstrahlung taken into account.

(C) The same as (B) but including the extra data obtained when the early cutoff in time is extended 3 mμsec earlier (Data II).

(D) The same as (C) but including internal radiative effects.

The fit to the experimental data is given in detail only for the last case (D) and may be seen in Fig. 18. The fit is very good, as can be judged from the figure and also from the values of χ^2 listed in Table V. Good fits were also obtained in all the other cases as well, showing that the shape is determined principally by the ionization loss and the response characteristics of spectrometer. The observations are evidently incapable of detecting the presence of the radiative effects from the shape alone. The different values of the integral J_π obtained in the cases studied reflect the contribution of the tail region below the main π-e peak. The effect is appreciable, about 20%, because of the high resolving power of the spectrometer.

Except for minor corrections the detection efficiency was the same for the μ electrons as for the π electrons so that in the ratio C_μ/C_π we need only take into account the different decay factors due to the different lifetimes of π and μ decay. The details of the calculation are summarized in Table VI.

As Table V shows the branching ratio was calculated using two different normalizations of the π-e data. This was because the π-e count required a delayed coincidence (23) which was switched off in the μ-e count. Any threshold difference in forming this coincidence would affect the π-e count but not the μ-e count. Accordingly, the experiment was designed to normalize the μ-e count to a count of μ-e events taken under precisely the same circuit conditions as were used in obtaining the π-e count. This was the case for the π-μ-e pictures. These were taken at the 450 ampere setting of the spectrometer at regular intervals between

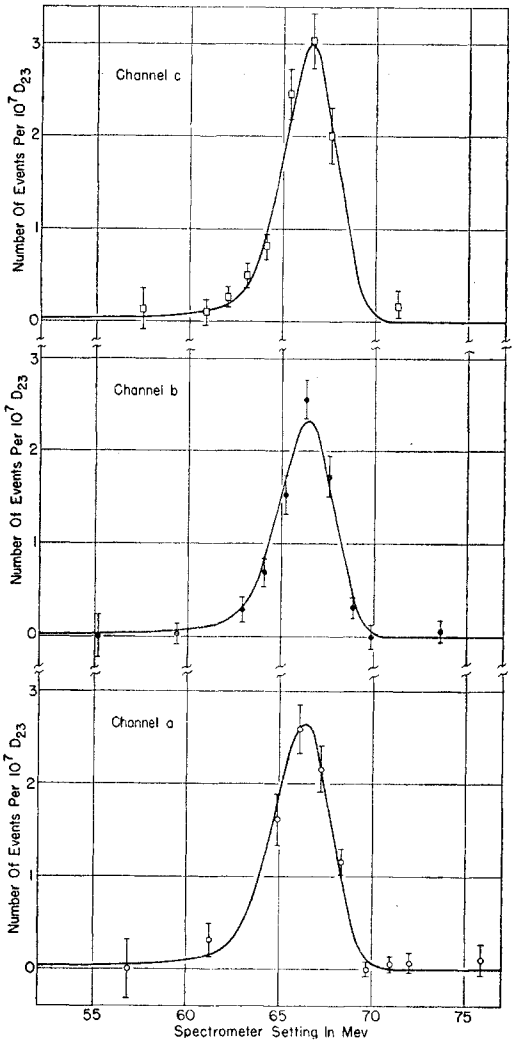

FIG. 18. Fits to the observed π-e events in three channels.

the π-e observations. The disadvantage here was that the small number of pictures which could be accumulated in the time available contributed to the statistical uncertainty of the final result.

The normalizations are summarized in the factors K and K' of Table VI. The agreement is good in the case of channels b and c, but marginal in the case of channel a. The values of the branching ratio for a using the π-μ-e pictures normalization seems anomalously high for this reason. Taking all the data together the agreement between the π-μ-e pictures and the μ-e count normalizations is quite good. The weighted mean $\bar{R}$ differs from $\bar{R}'$ by only 2%, well within the statistical expectations.

Possible loss of efficiency due to the action of the anticoincidence circuit was tested by comparing the results in (B) with that obtained when the lower cutoff T_1 was extended 3 mμsec giving the results in (C). The agreement is well within the statistics. In fact, these data give a slightly higher value for $\bar{R}$, supporting the view that the anticoincidence action is not yet depressing the result.

The fitting of the calculated curves to the experimental points was very sensitive to the energy calibration factor k. This turned out to be 0.9852 ± 0.0009; it would have been unity if the calibrations were correct. The 1.5% discrepancy is somewhat higher than we had expected, since the magnetic field measurements were good to better than 0.5%. However, other factors could have contributed to the discrepancy, among them saturation effects in the iron which became noticeable at the α-particle setting. Also, the centering of the stopping pions at the target might have been off and there might have been a systematic error in the ionization loss calibration. The energy calibration does not enter into the evaluation of the branching ratio directly. However, if one of the reasons given above were active, there would be some question as to the reliability of the overlap functions used in fitting the data.

To test the goodness of our overlap functions we took the view that the general shape was correct but that

TABLE VI. Detail of the branching ratio calculation. The branching ratio normalized to μ-e pictures is given by

$$f=\frac{J_\pi}{J_\mu}\frac{C_\mu}{C_\pi}\frac{N_\mu\cdot D_{23}{}^p}{N_\mu{}^p-A_\mu{}^p}=KJ_\pi.$$

The branching ratio normalized to μ-e integral is given by

$$f=\frac{J_\pi}{J_\mu}\frac{C_\mu{}'}{C_\pi}=K'J_\pi.$$

$J_\pi=\pi$-e integral per 10^7 D_{23} obtained by the least squares fit.

$J_\mu=\mu$-e integral $\int N_\mu dI/I$ per 10^7 D_{23}.

$C_\pi=\pi$-e time factor $(1/\tau_\pi)\int_{T_1}^{150}\exp(-t/\tau_\pi)dt$. $C_\mu=\mu$-e time factor for picture $=[1/(\tau_\mu-\tau_\pi)]\int_{T_1}^{150}[\exp(-t/\tau_\pi)-\exp(-t/\tau_\mu)]dt$. $C_\mu{}'=\mu$-e time factor for counting $=[1/(\tau_\mu-\tau_\pi)]\int_0^{150}\epsilon(t)\times[\exp(t/\tau_\mu)-\exp(-t/\tau_\pi)]dt$, where $\epsilon(t)$ is an efficiency factor due to anticoincidence cutoff. $N_\mu(450)=\mu$-e counts per 10^6 D_{23} at 450 amperes. $N_\mu{}^p=$number of pictures taken at 450 amperes. $A_\mu{}^p=$number of accidentals in $N_\mu{}^p$. $D_{23}{}^p=$number of monitor D_{23} in 10^6 required to obtain $N_\mu{}^p$.

Channel	a	b	c
J_μ	3605.7	3870.8	4558.0
$N_\mu(450)$	477±11	496±12	522±12
$N_\mu{}^p$ I[a]	425.5	486.5	565.0
$N_\mu{}^p$ II	434.5	491.5	577.0
$A_\mu{}^p$ I	14.5	14.5	17.0
$A_\mu{}^p$ II			
$D_{23}{}^p$	19.69	19.69	19.69
C_π I	0.4044	0.2951	0.3454
C_π II	0.4550	0.3321	0.3888
C_μ I	0.0500	0.0478	0.0490
C_μ II	0.0508	0.0487	0.0498
$C_\mu{}'$	0.9977	0.9966	0.9967
10^4K I	7.8359 ±4.8%	8.6584 ±4.5%	6.1731 ±4.2%
10^4K II	6.9242 ±4.8%	7.7567 ±4.5%	5.4540 ±4.2%
$10^4K'$ I	6.8423	8.7247	6.2209
$10^4K'$ II	6.0813	7.7527	5.6242

[a] Data I refer to the events for which the earlier cutoff time T_1 is 23.0 mμsec in channel a, 31.0 mμsec in b, and 27.0 mμsec in c. Data II refers to the events for which T_1 is reduced by 3 mμsec in each channel.

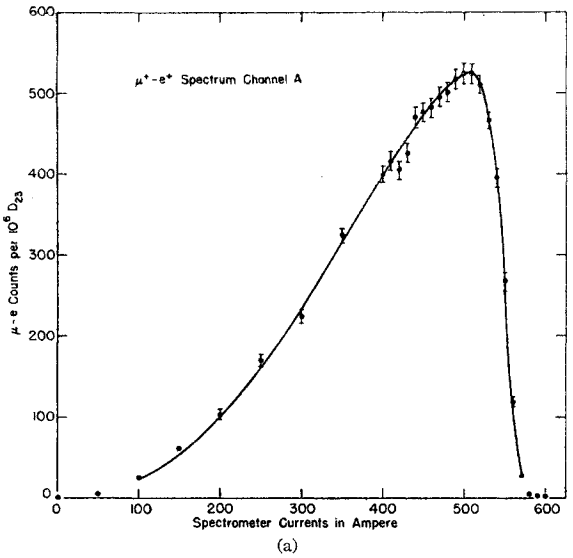

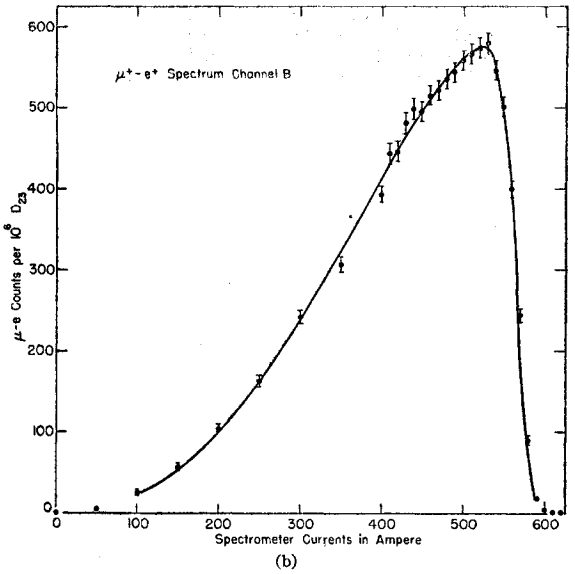

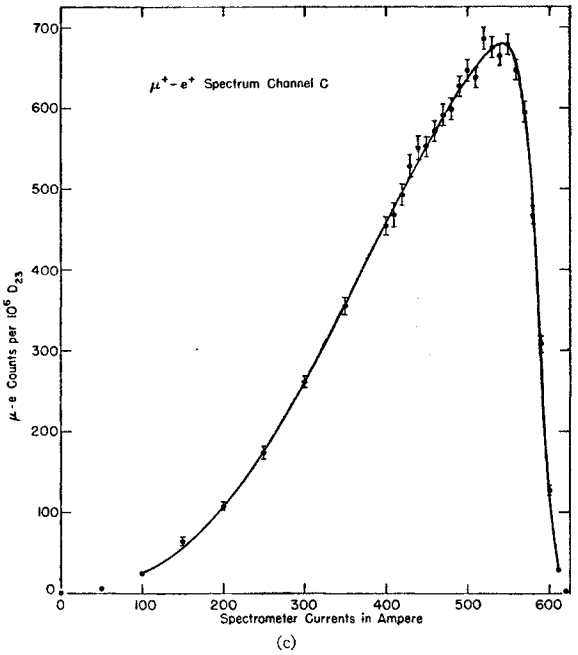

FIG. 19. Fits to the μ-e data.

the width might be in error. This would be the case, for example, if there were an error in the ionization loss calibration. We replaced E_0 in Eq. (12) by $E_0'=E_\pi-m(E_\pi-E_0)=k'W$ and looked for improved fits to the data according to the χ^2 minimum criterion by varying the two parameters m and k'. This reduces to the previous case, when $m=1$. Improved fits were obtained with $m=0.95$, $k'=0.987$ and gave $\chi^2=11.5$ (instead of 19.6). However, since there was no appreciable change in the value of the branching ratio, we reverted to the results already obtained but incorporated in the error the uncertainty implied by this analysis.

Another check on the validity of our procedures was provided by the fits we were able to obtain with the μ-e data. The calculation followed the lines already discussed for the fitting of the π-e data except that the Michel formula was used for the initial spectrum. Ionization loss, bremsstrahlung loss, and the response function of the spectrometer were folded in as before, but the fit was made by varying the Michel parameter as well as the energy calibration factor. As has been shown by Kinoshita and Sirlin[19] an adequate description of the distortion in the spectrum produced by internal radiative effects could be obtained with the Michel formula by modifying ρ; e.g., by taking $\rho=0.944\rho_M$. Since the statistical accuracy of the experimental points was considerably greater than for the π-e data a critical test could be expected. In this case the problem was coded, and the calculations carried out by means of an electronic computer. Good fits were obtained as can be judged from the plots of Fig. 19 with values of χ^2 quite close the accepted value. The results are tabulated in Table VII and show values of χ^2 well within the range expected from the number of experimental points fitted. The end point of the μ-e spectrum is given under the assumption that the energy varies linearly with the current and that $E_\pi=69.8$ Mev. The values obtained are in close agreement with those accepted. The sensitivity of the fit to the width of the resolution function was explored by varying this by 10% in either direction. An increase in the width such as would be the case if scattering at the slits and baffles were appreciable, actually worsened the fit; instead, as in the case of the π-e data, the fit improved somewhat

[19] T. Kinoshita and A. Sirlin, Phys. Rev. **113**, 1652 (1959). Our analysis here has not dealt adequately with the radiative corrections for the purpose of deriving a reliable value of ρ_M from these data.

TABLE VII. Parameters of μ-e spectrum determined by the χ^2 minimum method. The uncertainties shown are those derived from the fitting procedure and do not include other sources of error. The values of ρ_M are not to be taken as final measurements; they have not been adjusted for possible small systematic effects.

Channel	χ^2 Measured	χ^2 Expectation value	ρ_M	$E_{\mu\,\max}$ (Mev)
a	25.1	18	0.76±0.01	53.00±0.32
b	19.8	22	0.77±0.01	52.99±0.32
c	20.7	25	0.77±0.01	53.02±0.32

when the width was reduced. Additional details will be given in a subsequent paper which will deal with the problem of determining a reliable value of ρ from this and additional data. For the present purposes we conclude that scattering effects are unimportant and that the uncertainty in the knowledge of the response functions and ionization loss may amount to about 10% in the width. The uncertainty which this reflects in the branching ratio is less than 3%.

EARLIER FAILURE

In a previous communication from this laboratory[3] we reported our failure to observe the π-e decay mode. We have studied the previous experiment to determine the cause of the error. The old experimental result was based entirely on counter data. Delayed coincidences were used to count the number of π electrons in time intervals extending roughly from 25–45, 50–70, and 75–95 mμsec after a pion stopped in the target counter. The counter data were analyzed in two steps. First, a crude analysis which utilized the counting rate in the first time interval alone indicated that the branching ratio was 5×10^{-5}. Second, to get more detailed information, the counts in the three time intervals were analyzed for the presence of a component decaying with the 25.6 mμsec pion lifetime superimposed on the background.

As in the present experiment, both the stopping pion and the emerging electron produced pulses in the target counter. Normally, the pion pulse was much larger than the electron pulse. The logical arrangement of the circuits required that the electron pulse be clearly distinguishable from the pion pulse. To see the electron at short times after the pion required correct design and adjustment of the clipping lines together with careful setting of the photomultiplier voltages and associated circuitry to avoid overshoot, saturation effects and pulse lengthening with large pulses. In the absence of continuous photographic monitoring and the possibility of having a visual check of each event such as was used in the present experiment, a maladjustment could go by for some time unnoticed. We now believe that our coincidence circuits missed a large fraction of the electron pulses which should have activated the first channel.

We have verified that this was the principal cause of our failure to observe π-e events by re-analyzing the data in the second and third channels alone, rejecting completely the data of the first channel. This gave a positive result not inconsistent with our present evidence.

RESULTS

A number of small corrections should be considered before giving the final results. The annihilation in flight of the positive electrons, an important consideration in some experiments which deal with these particles, is inconsequential here because of the small amount of matter which they have to traverse to be detected. Moreover, the losses occur almost equally for the μ electrons and for the π electrons and so cannot influence the branching ratio in this case. Such a cancellation does not occur in the case of the Bhabha scattering. This removes electrons from the π-e peak, but in the μ-electron distribution the losses only reappear at some lower energy and are not missed in the integral. In this sense the behavior is similar to the bremsstrahlung. This effect may be included in the constant of formula (2) which gives the bremsstrahlung loss. This depends on the average ionization loss for positive electrons in scintillator material and we have already remarked that our choice of 2.00 Mev/(g/cm^2) for this might have been too high. A rough estimate showed that a reduction in this constant by about 10% would account for the effects alluded to. This implies an increase in the branching ratio by about (2±1)%. There is another correction which acts in the opposite sense. This is the loss of muons which can escape from the target before they decay. The loss depends on where pions stop in the target. Because the range of the muons is only 1.4 mm, the magnitude of the effect is small and a rough estimate places it at (2±2)%.

The branching ratio may be obtained from the weighted mean value, $(1.178\pm0.051)\times10^{-4}$ of Table V, which resulted from the χ^2 minimum fit once both internal and external radiative effects had been taken into account and the normalization to the μ-e pictures data made. This does not take into account those π electrons whose energy differs from E_π by more than 10 Mev. Kinoshita[7] has shown that these amount to 2.45% so that the value above should be increased by this amount if the total branching ratio is to be given. The value of the branching ratio is not altered by the corrections discussed above; these affect only the uncertainty in the result. The value 0.051 for the uncertainty just given resulted from the χ^2 minimum analysis; it is entirely due to the statistical limitations of the data. It is reassuring to notice that the spread of the values obtained from the different channels, considering these as yielding three separate independent measurements reflects almost the same uncertainty. Our final value for the branching ratio must include the uncertainty in the knowledge of the ionization loss and of the resolution width of the spectrometer. As discussed

above this amounts to about 3% in the branching ratio. Combining all these effects we give as our final value for the branching ratio of the electronic mode in the decay of the positive pion, $(1.21\pm0.07)\times10^{-4}$.

DISCUSSION

According to Kinoshita[7] the branching ratio should be 1.23×10^{-4} once radiative effects are taken into account and all decay electrons counted. This is quite close to our result. Berman[6] has given the following formula for the branching ratio if only electrons with energies differing from E_π by less than ΔE are considered,

$$f=\left(11.00+0.27\ln\frac{2\Delta E}{m_e}\right)\times10^{-5}.$$

ΔE corresponds to $\eta_2=10$ Mev in our analysis so that Berman's formula gives $f=1.20\times10^{-4}$, to be compared with our experimental value $(1.18\pm0.07)\times10^{-4}$ for this case. This experiment, which compares directly the muon with the electron couplings insofar as they enter in pion decay, provides a strong confirmation of the hypothesis of a universal V-A interaction of Fermi couplings. From the point of view of the five possible Fermi couplings only two, the axial vector and the pseudoscalar, can enter in the nonradiative pion decay because of the pseudoscalar character of this particle. The observed branching ratio is fully accounted for by the axial vector part of the interaction; it is 2×10^{-5} as large as it would be if the decay of the pion were governed by the pseudoscalar interaction. Thus, the experiment provides the strongest evidence known at present against the existence of a direct pseudoscalar component in the universal Fermi interaction.

With respect to the validity of the radiative corrections, the experiment would have given $(1.13\pm0.08)\times10^{-4}$ for the branching ratio if these corrections were not included. This would have to be compared with a ratio of 1.28×10^{-4} on the basis of a universal Fermi interaction theory with electromagnetic corrections neglected. Thus, the experiment supports the existence of these effects, albeit not in a very decisive way.

ACKNOWLEDGMENTS

We are pleased to thank Dr. Paul Fields and Ray Brown for preparing the plutonium α-particle sources used in calibrating the spectrometer, and Paul Kliauga and Dave Dwoskin for their help in measuring the oscilloscope traces. We also thank Dr. Allan Segar and Charles Rey for their help in checking the magnetic field calibrations using novel Hall effect and magneto-resistance probes. One of us, HLA, offers his apologies to those who took seriously the first negative result and tried uselessly to explain it, and also to those who because of it gave up or postponed their own attempts to discover the π-e process. The groups at CERN and at Columbia whose insight and conviction caused them to perservere in their own experiments have already been rewarded by the successful outcome and importance of their labors.

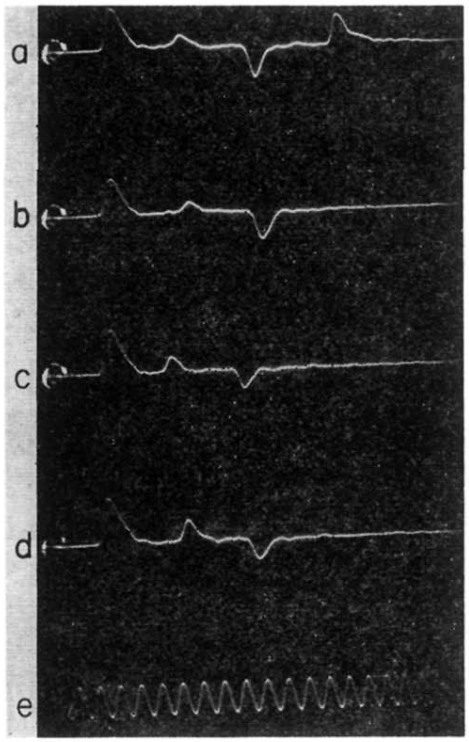

(a)

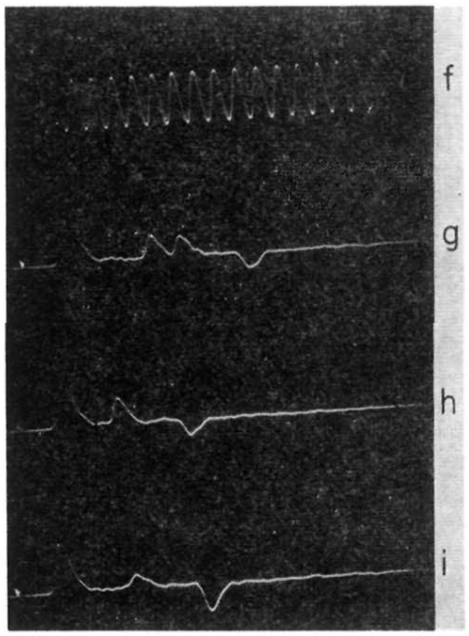

(b)

FIG. 8. Photographs of π-e events taken at 760 amperes. Traces b, c, d, h, and i are normal πe events; an event of type $\pi e(+)$ is shown in a and of type $\pi(+)e$ in g. The 100-megacycle timing wave is shown in e and f.

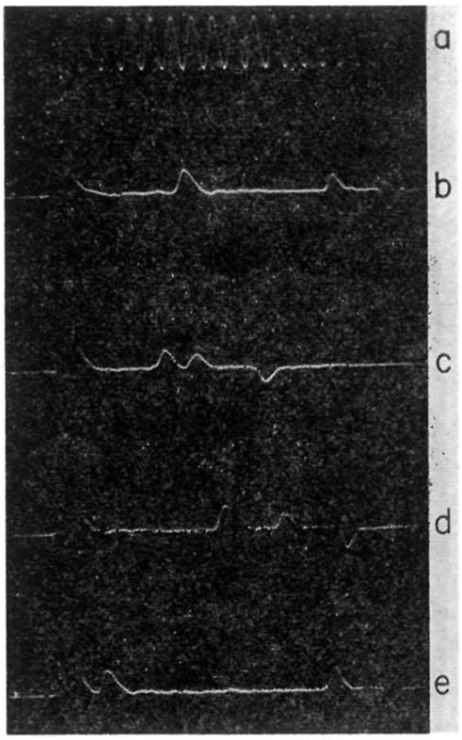

FIG. 9. Photographs of π-μ-e events taken at 450 amperes. The 100-megacycle timing wave is shown in a.